

Comparison of the $\nu=1$ and $\nu=2$, $J=1\rightarrow 0$ SiO masers toward TX Cam

Ioannis Gonidakis*

CSIRO Astronomy and Space Science, Vimiera and Pembroke Roads, Marsfield NSW 2122, Australia

E-mail: ioannis.gonidakis@csiro.au

Phil Diamond

CSIRO Astronomy and Space Science, Vimiera and Pembroke Roads, Marsfield NSW 2122, Australia

E-mail: phil.diamond@csiro.au

Athol Kemball

Department of Astronomy, University of Illinois at Urbana-Champaign, 1002 W. Green Street, Urbana, IL 61801, USA

E-mail: akemball@illinois.edu

The extended atmospheres/inner circumstellar envelopes of Asymptotic Giant Branch stars are very complex regions where intense phenomena occur and periodic passages of shock waves are believed to contribute to their complexity. Located between the extended atmosphere and the dust formation zone, SiO masers provide a valuable tool in the study of these complex regions. Registration of the relative positions of the $\nu=1$ and $\nu=2$, $J=1\rightarrow 0$ emissions can help us compare the characteristics of these transitions; such comparisons can greatly contribute in our understanding of the physical conditions and kinematics in the extended atmosphere of the star. We will present results from a long-term monitoring campaign of both emissions. Our data cover 0.6 cycles of the stellar pulsation. Observations were conducted with the VLBA once every month.

*11th European VLBI Network Symposium & Users Meeting,
October 9-12, 2012
Bordeaux, France*

*Speaker.

1. Introduction

Silicon monoxide (SiO) masers are located in the extended atmosphere of late-type stars, between the stellar atmosphere and the dust-formation zone [5][16]. By virtue of their position they are a valuable tool in studying the properties of this complex region.

There are two proposed mechanisms for the pumping of SiO masers. The first suggests that SiO masers are radiatively pumped [2], with collisional pumping contributing marginally to the total output. The model predicts that maser lines from different vibrational states require different physical conditions, thus they should be located at different stellar radii. On the other hand, collisional pumping models [11] can operate under a wide range of physical properties and maser features could overlap. According to the model, radiative pumping, although unlikely to be the primary pumping mechanism, cannot be ruled out; it can be the primary pumping mechanism of certain features.

A number of studies have been conducted with interferometric techniques; simultaneous observations of SiO masers from different vibrational states, different rotational transitions and isotopomers were used to study the pumping mechanism of SiO masers, by examining the spatial coincidence of the maser spots [3][12][15][17]. It was soon revealed that the spatial coincidence of the spots alone is not sufficient to explain the pumping mechanism of the masers. Collisional pumping models [8] can explain the similar distributions of the maser spots; however, the inclusion of the effects of water line overlaps in the radiative pumping model [15] can also produce the observed similarities.

2. Observations and Data Reduction

The data used for this study are part of the long-term monitoring of the SiO masers toward TX Cam [4][6][7]; for this campaign, the 10 Very Long Baseline Array (VLBA¹) antennas and 1 antenna from the Very Large Array (VLA) were used. The $\nu=1, J=1\rightarrow 0$ line was observed from the 24th of May 1997 until the 9th of September 1999 in biweekly intervals; observations were then switched to monthly intervals until the 25th of January 2002. The whole project covers three complete pulsation cycles of TX Cam, from $\phi\sim 0.68$ to 3.74. However, the $\nu=2, J=1\rightarrow 0$ line was included only after the 9th of September 1999, covering phase from $\phi\sim 2.18$ to 3.74. This is the most detailed simultaneous monitoring of these two maser lines with interferometric techniques to date. Table 1 lists the data used in this paper, covering phases $\phi\sim 3.08$ to 3.68.

The $\nu=1$ and $\nu=2, J=1\rightarrow 0$ transitions were observed at rest frequencies of 43.122027 and 42.820587 respectively, centred at an LSR velocity of -9 km s^{-1} . Data were recorded in dual polarisation over a 4MHz bandwidth and correlated with the VLBA correlator in Socorro. Datasets of 128 channels were created for all four cross-polarisation pairs, with nominal spectral resolution of 31.25 kHz, corresponding to a velocity resolution of 0.217 km s^{-1} .

Data analysis was based on previously used techniques [9][10], with the AIPS package. The result for each dataset was a 128-channel cube of 1024×1024 pixels on the projected plane of the sky, with pixel separation of 0.1 mas. The need to self-calibrate, introduced problems due

¹The Very Long Baseline Array (VLBA) is operated by the National Radio Astronomy Observatory (NRAO), a facility of the National Science Foundation (NSF) under cooperative agreement by Associated Universities, Inc.

Epoch	Observing date	Phase	Epoch	Observing Date	Phase
BD69H	2001 January 20	3.08 ± 0.01	BD69N	2001 August 16	3.45 ± 0.01
BD69I	2001 February 18	3.13 ± 0.01	BD79A	2001 September 28	3.53 ± 0.01
BD69J	2001 March 16	3.18 ± 0.01	BD79B	2001 October 12	3.55 ± 0.01
BD69K	2001 April 15	3.23 ± 0.01	BD79C	2001 November 12	3.61 ± 0.01
BD69L	2001 May 19	3.29 ± 0.01	BD79D	2001 December 18	3.67 ± 0.01
BD69M	2001 June 24	3.36 ± 0.01	BD79E	2002 January 25	3.74 ± 0.01

Table 1: The code names, date of observation and the pulsation phase of TX Cam for the epochs used in this study.

to the loss of information of the absolute position of the final maps. We followed well-established techniques for both the alignment of the maps from one epoch to the next [4][6][7], and the accurate registration of the maps of the two transitions [1].

3. Results

Fig. 1 shows the total intensity and velocity maps of the two transitions for epoch BD69I; results are similar for all the other epochs in this dataset. SiO masers from both transitions form rings of emission around the star. The overplotted total intensity maps show a high degree of overlapping between the maser features of the two transitions. The $\nu=2, J=1 \rightarrow 0$ emission appears to be less extended and covering a smaller part of the ring's perimeter. Most of the $\nu=2, J=1 \rightarrow 0$ spots have a $\nu=1, J=1 \rightarrow 0$ counterpart.

This coincidence is not only apparent in their spatial distribution but also in their radial velocity characteristics. The coincident spots appear to have the same kinematic behaviour along the line of sight, although the $\nu=1, J=1 \rightarrow 0$ emission appears to have an additional arc of blue-shifted features in the western part of the ring that are not present at $\nu=2, J=1 \rightarrow 0$.

For the determination of the inner shell boundary radius and the width of the ring, we used a previously successfully applied technique [7]. Fig. 2a plots the inner shell boundary radius as a function of stellar phase. It is apparent that the changes in the radii of the rings follow the same pattern. In line with all other results and theoretical models, the $\nu=2, J=1 \rightarrow 0$ is located closer to the star. The distance at which the inner shell boundary forms, is found to be between 10 and 11.5 mas, i.e. 3.9-4.5 a.u. from the centre of the star, assuming a distance of 390 pc for TX Cam [13].

Fig. 2b plots the width of the ring as a function of the stellar phase. The less extended nature of the $\nu=2, J=1 \rightarrow 0$ is apparent; however there is no obvious correlation between the change in the widths and their relative sizes with the stellar phase.

Fig. 3 is a collage showing the evolution of maser spots and their kinematic behaviour in the plane of the sky (proper motions). Each row corresponds to a different epoch, arranged in chronological order from top to bottom; left and right columns are the total intensity maps of the $\nu=1, J=1 \rightarrow 0$ and $\nu=2, J=1 \rightarrow 0$ transitions respectively. For simplicity, not all epochs are included in this collage. A movie, showing the kinematics and evolution of the maser spots, was also created from these data and served as a visual aid for the comparison of the two emissions. The most prominent result is that, maser spots from both transitions have the same kinematic characteristics

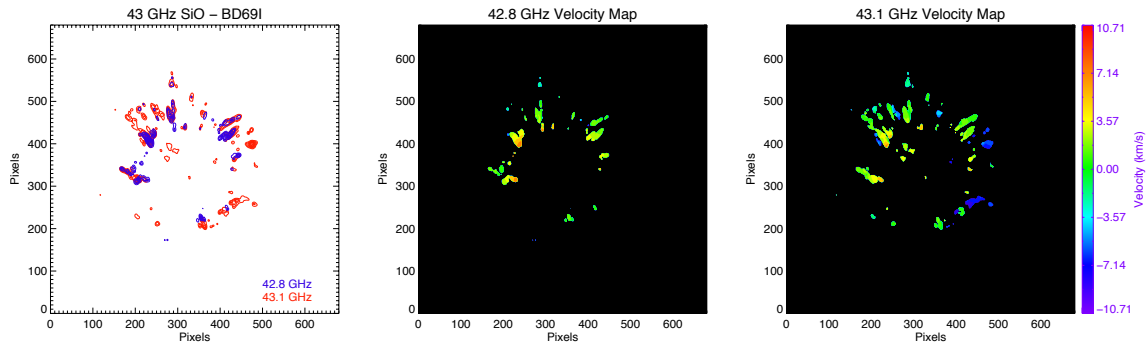


Figure 1: Epoch BD69I. *Left*: Aligned maps of the $\nu=2, J=1 \rightarrow 0$ (blue) and $\nu=1, J=1 \rightarrow 0$ (red) SiO masers. *Middle*: Velocity map of the $\nu=2, J=1 \rightarrow 0$ masers. *Right*: Velocity map of the $\nu=1, J=1 \rightarrow 0$ masers.

in the plane of the sky. Combined with the radial velocity characteristics, we conclude that the three-dimensional behaviour of the overlapping spots is identical. This might suggest that these features arise from the same volume of gas in both transitions and do not appear to coincide due to projection effects taking place.

According to previous studies on TX Cam [4][6][7], despite the overall ordered motion of the ring, there are features that deviate from this behaviour and appear to be peculiar kinematically. Such a feature is included in this dataset and is located at the northern part of the ring. The feature, in both transitions, appears to fall toward the star and then bounce, changing the direction at which it is moving. It would be very interesting to see whether the kinematics of this feature could be explained by the existence of shocks in the extended atmosphere. Thus, in Fig. 3 we also included a shock wave that, as expected by models, is created once per stellar cycle [8] and propagates outward with a velocity of 7 km s^{-1} [14]. It appears that the proposed shock could be responsible for this peculiar kinematic behaviour, since its passage coincides with the bounce of the feature. Moreover, the influence of the shock in the structure of the feature is also evident in the last frames of the movie; the feature becomes elongated and then it breaks down to smaller feature as the shock propagates through it. It then disappears once the shock leaves the region. This is an additional indication that both transitions arise from the same volume of gas and do not appear coincident due to projection. Our data might be revealing the importance of shock waves and their contribution in the observed properties of the SiO masers toward Mira Variables.

4. Conclusions

The $\nu=1$ and $\nu=2, J=1 \rightarrow 0$ SiO masers toward TX Cam are located in rings with similar structures around the star. The $\nu=2, J=1 \rightarrow 0$ ring is located closer to the stellar surface and is less extended. There is no evidence of a dependence of these properties with the stellar pulsation phase, however, results from the whole monitoring campaign, covering 1.5 stellar cycles, will be more conclusive. For the features that coincide in both transitions, it appears that this is not due to projection effects; they arise from the same volume of gas since they have the same three-dimensional

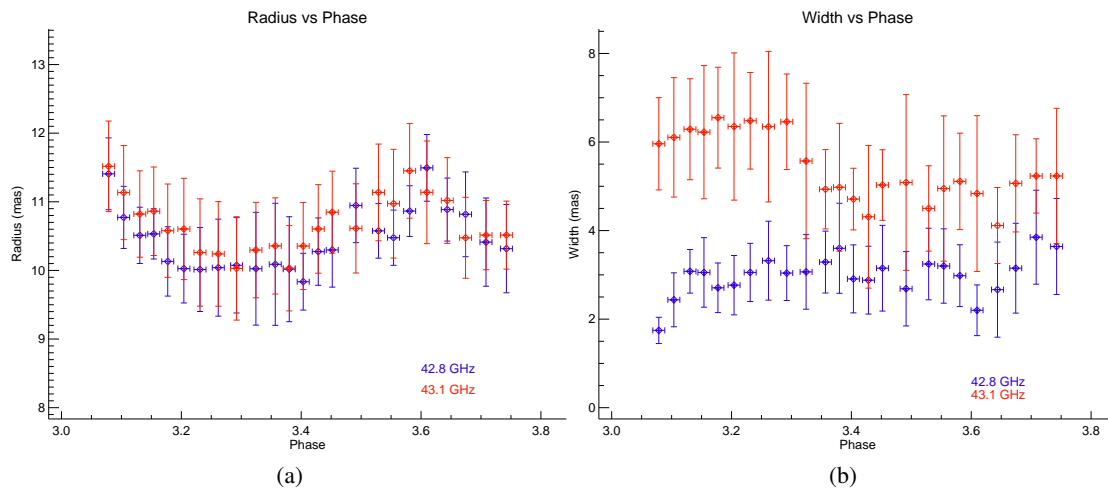


Figure 2: *Blue*: $\nu=2, J=1 \rightarrow 0$ - *Red*: $\nu=1, J=1 \rightarrow 0$. (a) The inner shell radius plotted as a function of stellar pulsation. (b) The width of the ring plotted as a function of stellar pulsation.

velocity characteristics. The behaviour of some features can be explained by the passage of a shock wave through the masering zone.

References

- [1] Boboltz D. A., Wittkowski M., 2005, *ApJ*, **618**, 953
- [2] Bujarrabal V., 1994, *A&A*, **285**, 953
- [3] Desmurs J. F., Bujarrabal V., Colomer F. and Alcolea J., 2003, *A&A*, **360**, 189
- [4] Diamond P. J. and Kemball A. J., 2003, *ApJ*, **599**, 1372
- [5] Elitzur M., *Astronomical Masers*, Kluwer Academic Publishers, 1992
- [6] Gonidakis I., Diamond P. J. and Kemball A. J., 2010, *MNRAS*, **406**, 395
- [7] Gonidakis I., Diamond P. J. and Kemball A. J., 2013, *MNRAS*, in preparation
- [8] Gray M. D., Wittkowski M., Scholz M., Humphreys E. M. L., Ohnaka K. and Boboltz D., 2009, *MNRAS*, b394, 51
- [9] Kemball A. J., Diamond P. J., 1997, *ApJ*, **481**, 111
- [10] Kemball A. J., Diamond P. J., Cotton W. D., *A&AS*, **110**, 383
- [11] Lockett P., Elitzur M., 1992, *ApJ*, **399**, 704
- [12] Miyoshi M., Matsumoto K., Kameno S., Takaba H and Iwata T., 1992, *Nature*, **395**, 371
- [13] Olivier E. A., Whitelock P. and Marang F., 2001, *MNRAS*, **226**, 490
- [14] Reid M. J. & Menten K. M., 1997, *ApJ*, **476**, 346
- [15] Soria-Ruiz R., Alcolea J., Colomer F., Bujarrabal V., Desmurs J. F., Marvel K. B. and Diamond P. J., 2004, *A&A*, **426**, 131
- [16] Wittkowski M., Boboltz D.A., Ohnaka K., Driebe T., and Scholz M., 2007, *A&A*, **470**, 191
- [17] Yi J., Booth R. S., Conway J. E. and Diamond P. J., 2005, *A&A*, **432**, 531

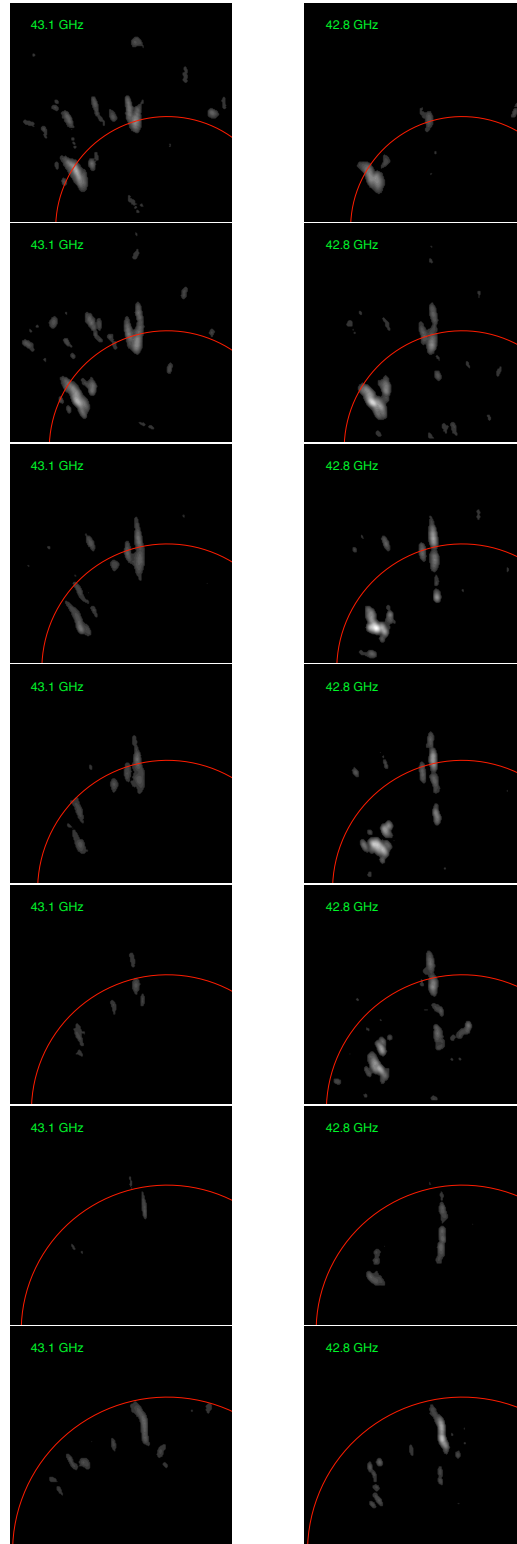


Figure 3: A collage, showing the evolution, kinematic behaviour and correlation with a shock wave of the NE part of the SiO maser ring for both $\nu=1, J=1 \rightarrow 0$ (left) and $\nu=2, J=1 \rightarrow 0$ (right) SiO masers. Of particular interest is the bouncing feature in the northern part of the ring that appears to have the same behaviour in both transitions. The epochs plotted from top to bottom are BD69H,J,L,M,N and BD79C,D